Research Article

Tao Meng*, Kanjun Ying, Yongpeng Hong, and Qinglei Xu

Effect of different particle sizes of nano-SiO_2 on the properties and microstructure of cement paste

https://doi.org/10.1515/ntrev-2020-0066
received July 15, 2020; accepted August 05, 2020

Abstract: Nano-materials modified cement-based materials have attracted wide attention due to their advantages of improving strength and durability. In this paper, the effect of nano-SiO_2 (NS) with particle sizes of 15 and 50 nm on the mechanical properties and microstructure of cement paste was studied. The results showed that 50 nm NS provided a greater compressive strength than that of 15 nm NS, while 15 nm NS afforded a denser microstructure than that of 50 nm NS. A fluctuation in the compressive strength was revealed using a physico-chemical reaction equation, and the microstructure was interpreted by a pore structure analysis. In addition, the orientation index of calcium hydroxide (CH) with 15 nm NS could be reduced significantly in the early stages (the early stages refer to the first three days from the maintaining of specimens) compared with when the 50 nm NS was used. The experimental results also showed that NS helped increase the mechanical strength of cement paste, advance the endothermic peak of CH, and refine the size of the CH crystals. The microstructural changes at different stages of cement paste with different particle sizes of NS were investigated by X-ray diffraction, scanning electron microscopy, mercury intrusion porosimetry and differential thermal analysis. This study is expected to promote the research and application of nano-materials in the cement industry by clarifying the performance of NS with different particle sizes.

Keywords: nano-SiO_2, particle size, mechanical properties, microstructure, cement paste

*** Corresponding author: Tao Meng,** Institute of Engineering Materials, College of Civil Engineering and Architecture, Zhejiang University, Hangzhou, 310058, China, e-mail: taomeng@zju.edu.cn
Kanjun Ying, Yongpeng Hong, Qinglei Xu: Institute of Engineering Materials, College of Civil Engineering and Architecture, Zhejiang University, Hangzhou, 310058, China

1 Introduction

Nanotechnology has had a great impact on the development of chemistry, physics and materials and has become one of the most novel sciences with useful applications owing to its use of extremely small particles [1,2]. For concrete studies, applied nano-materials are recommended to be not more than 100 nm in size.

Recent studies have revealed that the incorporation of nano-SiO_2 (NS) has a significant effect on the workability, mechanical properties and durability of cement-based materials owing to its small particle size and special surface properties [3–5]. Whether it is used for cement paste or mortar, the incorporation of NS will reduce their fluidity [6,7]. Senff et al. [8] indicated that the decrease in the fluidity was in accordance with one hypothesis that the presence of NS decreased the amount of lubricating water available within the inter-particle voids; this phenomenon could lead to an increase in the yield stress and plastic viscosity of concrete. The decrease in the fluidity value is also due to the greater water requirement for a standard consistency of cement paste, which increases with the total surface area of NS [9]. In addition, NS is beneficial to the compressive and flexural strength of cement-based materials, and these strengths are also enhanced with an increase in the NS content [10,11]. Furthermore, the permeability and frost and corrosion resistance can also be modified by the incorporation of NS [12,13]. The micromorphology of the interfacial transition zone seems to be more compact and homogeneous for concrete containing NS, as observed through scanning electron microscopy (SEM) [14,15]. In addition, mercury intrusion porosimetry (MIP) results revealed that the pore size distribution became refined, which may be helpful in reducing the ingress rate of water and chloride ions.

Normally, it is believed that the filling effect, high activity, and seeding effect are the three main reasons for

Open Access. © 2020 Tao Meng *et al.*, published by De Gruyter. This work is licensed under the Creative Commons Attribution 4.0 International License.

the property modification of cement-based materials combined with NS. The filling effect can make the structure more compact, and high activity is beneficial for improving the mechanical properties and durability. Nanoparticles also provide a seed of a nucleation site for the precipitation of C–S–H gels, which may accelerate the hydration of cement and trigger the potential activity of mineral admixtures [13,16,17]. In addition, further research about the nano-effect has been reported in recent years. Kooshafar et al. [18] found that the morphology of nano-silica could influence various properties of cement mixes, which may be attributed to the changes in the growth space of CH and size of CH crystals. Xu et al. [19] showed that the hydration degree of C_3S was accelerated before 3 days but slowed later with an increase in the NS content.

The effects of different particle sizes of NS on the properties of cement-based materials at early ages have not yet been studied, which may greatly block the application of nano-materials in the cement and concrete industry. We know that smaller NS particles have a larger specific surface area and higher activity. Land and Stephan [20] found that NS with a particle size of 7 nm could provide more hydration heat than that with a particle size of 86 nm, thereby indicating that particle size has an important influence on the properties of cement-based materials. However, researchers have found that nanomaterials with large particle sizes had greater compressive strength. NS with a particle size of 40 nm has greater compressive strength than NS particles with sizes of 12 and 20 nm in mortars [21]. NS particles with a size of 80 nm provide greater compressive strength than those with a size of 15 nm in concrete [22]. This phenomenon is contradictory to common perception. Furthermore, cement pastes with smaller NS particles have a denser structure. However, Givi et al. [23] found that the performance of 80 nm SiO_2 was better than that of 15 nm SiO_2 in improving the water penetration resistance of concrete. Haruehansapong et al. [24] showed that 40 nm NS was the optimum size and provided the highest abrasion resistance. Smaller NS particles (12 and 20 nm) will lead to shrinkage and cracking of the cement mortar and decreased bond strength. This reveals that the research results on the effect of NS particle size on the performance and mechanism of cement-based materials are quite different. However, almost all the relevant studies were focused on the middle and late stages of hydration, thereby leading to unclear differences in the performance of NS with different particle sizes in the early stages of hydration.

In this study, two different particle sizes of NS (15 and 50 nm) are considered to study the effect on the mechanical properties, micromorphology and pore structure of cement pastes, particularly in the early stages. MIP, X-ray diffraction (XRD), SEM, and differential thermal analysis (DTA) are used to reveal the mechanisms of different effects under different particle sizes. This study can provide key insights into the effects of different sizes of NS on the properties and microstructure of cement-based materials at early ages.

2 Materials and experimental methods

2.1 Materials

Ordinary Portland cement (P.O. 42.5) and tap water were used for the test. VK-SP15 and VK-SP50 NS powders were produced by Hangzhou Wanjing New Material Co., Ltd were selected as the nano-materials. The technical specifications of the NS powders are listed in Table 1.

2.2 Preparation of cement paste

The mixture proportions of cement paste specimens are listed in Table 2. The cement was mixed slowly in a mixer for 120 s, let stand for 15 s, and then mixed quickly for 120 s. The cement paste was then poured into six-joint copper moulds of 20 mm × 20 mm × 20 mm and consolidated by a vibration table. The specimens were maintained at a constant temperature of 20°C for 24 h. After being demoulded, the specimens were kept under the standard curing conditions (temperature of 20 ± 2°C and relative humidity of 95% or greater) until the testing stage.

2.3 Experimental methods

2.3.1 Fluidity

The cement paste was poured into a conical mould in the form of a frustum according to GB/T8077-2012 [25]. During the test, the cone was lifted straight up to allow a

Table 1: Technical specifications of NS

Specimen	Appearance	Average particle size/nm	Specific surface area/m^2/g	PH value
NS15	White powder	15 ± 5	250 ± 30	5–7
NS50	White powder	50 ± 5	200 ± 30	5–7

Table 2: Mix proportion of specimens (wt%)

Specimen	Cement	NS15	NS50	Water
JZ	100	—	—	37
N-15	98	2	—	37
N-50A	97.5	—	2.5	37
N-50B	98	—	2	37

Note: the specific surface area of N-50A is similar to that of N-15. "JZ" means a blank control group. Based on the literature review and previous experiments, we determined that the optimal incorporation of NS was about 2 wt%.

free flow of the paste without any jolting, and two diameters perpendicular to each other were determined. Their mean value was regarded as the fluidity of the designed cement paste.

2.3.2 Compressive strength test

The compressive strength of the cement paste was measured at 1, 3 and 28 days using a compressive testing machine (WDW-100) according to GB/T50081-2002 [26]. The average value of the three samples was reported.

2.3.3 Microhardness analysis

The cement paste specimens cured for 1, 3 and 28 days were first ground and polished. Finer grades of abrasive papers were then employed until the interface was smooth enough. A Vickers hardness tester (DHV-1000) was used with 0.1 kgf and 15 s dwelling time. Twelve data points were collected from each sample and the average value was calculated.

2.3.4 XRD analysis

The cement paste specimens for XRD were kept at 20°C, and the hydration was stopped by pure alcohol after 1, 3 and 28 days. Before the test, the cement paste specimens were broken and ground on a 45 mm sieve to a residue ratio of less than 2%. The mineralogical investigations were performed by XRD analysis using a PANalytical Empyrean XRD Instrument and Cu Kα X-ray radiation source. The step size was 0.026°, the acceleration voltage was 40 kV, and the 2θ scanning range was 10–80°.

2.3.5 SEM analysis

The cement paste specimens for SEM were moulded and kept at 20°C before they were broken into small fragments at 1 day. These small fragments were sprayed with gold for 60 s in an SBC-12 small particles sputtering apparatus to make the specimens conductive. The microscopic morphology of the specimens under different magnifications was observed using a Gemini SEM300.

2.3.6 Pore structure analysis

MIP is considered a high-precision method for analysing the micropore structure of materials. The cement paste specimens cured for 1 day for MIP were broken into small fragments after the compressive strength test and dried in an oven at 60°C for 48 h before the test. The MIP test was conducted using an AutoPore IV 9500. The wetting angle of mercury to solids (θ) was 130°, and the surface tension of mercury (σ) was set to 485 dynes per cm.

2.3.7 DTA

The samples were the same as those for the XRD analysis. Powdered samples were tested under a nitrogen atmosphere with a sample mass of approximately 8 mg. They were heated from 20°C to 900°C with a constant heating rate of 10°C/min. The degree of hydration was analysed by reading the peak area in the curve. The DTA test was investigated by using an SDTQ600.

3 Results and discussion

3.1 Fluidity

The effect of NS with particle sizes of 15 and 50 nm (simplified to 15 and 50 nm NS) on the fluidity of cement paste specimens is summarized in Table 3. The results indicated that the fluidity of the cement paste was clearly decreased by NS. For specimen JZ, the fluidity value of the reference sample was 90 mm, which decreased sharply to almost 60 and 65 mm when 2.0% and 2.5% NS were added, respectively. Compared with that of the specimen N-50A and specimen N-50B, specimen N-15 showed greater fluidity reduction.

3.2 Compressive strength

The compressive strength of cement paste specimens is shown in Figure 1. The results indicated that the incorporation of NS helped to improve the compressive strength of the cement paste, particularly at early age.

Table 3: Effect of NS on the fluidity of specimens (mm)

Specimen	JZ	N-15	N-50A	N-50B
Fluidity	90	60	60	65
Standard deviation	1	0	0	3

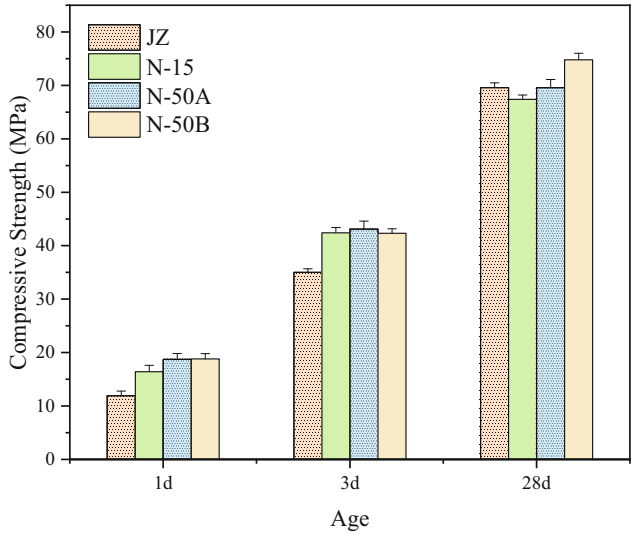

Figure 1: Compressive strength of specimens.

The compressive strength of specimen N-15 was 38% higher at 1 day and 20% higher at 3 day than that of specimen JZ, while that of specimen N-50 increased by 57% at 1 day and by 23% at 3 days. As for the strength at later ages, it seemed that NS had no clear effect. In the later stages, the compressive strength of the cement paste decreased with the incorporation of 2% 15 nm NS. Therefore, the improvement of the cement paste strength by NS was reflected in the early stage, and the incorporation of NS delayed the strength development at a later age.

It seemed that 50 nm NS presented a greater effect on the compressive strength than that of 15 nm NS. The compressive strengths of specimen N-50A were 14.0% and 3.3% greater than those of specimen N-15 at 1 and 28 days, respectively. The compressive strengths of specimen N-50B increased by 14.6% and 11.0% when compared with those of specimen N-15 at 1 and 28 days, respectively. According to the formula postulated by Porter and Easteriing [27] and Muller [28], the critical radius of nucleation (r^*) is defined as follows:

$$r^* = \frac{2\gamma_{sg}}{\Delta G_V} \tag{1}$$

where γ_{sg} and ΔG_V depend on the particle composition and are equal for different particle sizes. Therefore, most of the nucleation sites in the 15 nm NS were difficult to grow because they did not reach the critical radius, thereby resulting in a discontinuity in the generated C–S–H gel, which affected the later strength [22]. Meanwhile, the compressive strength results of specimen N-50A and N-50B at 28 days did not support the concept that more is better, and a reasonable NS content could contribute to the development of strength.

3.3 Microhardness analysis

The microhardness of cement paste specimens is shown in Figure 2. The results indicated that NS helped to improve the microhardness in the early and later stages. For example, the microhardness values of specimen N-15 were 21.1%, 13.8% and 7.6% greater than those of specimen JZ at 1, 3 and 28 days, respectively. The reason for the improvement in microhardness might be the incorporation of NS which helped to increase the density of the microstructure. Meanwhile, the microhardness values of specimen N-15 were 17.7% and 14.0% greater than those of specimen N-50 at 1 and 3 days, respectively. The results showed that 15 nm NS could

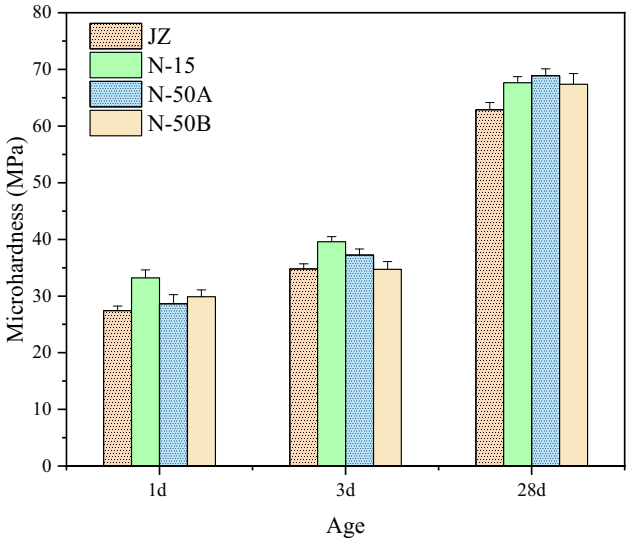

Figure 2: Interface microhardness of specimens.

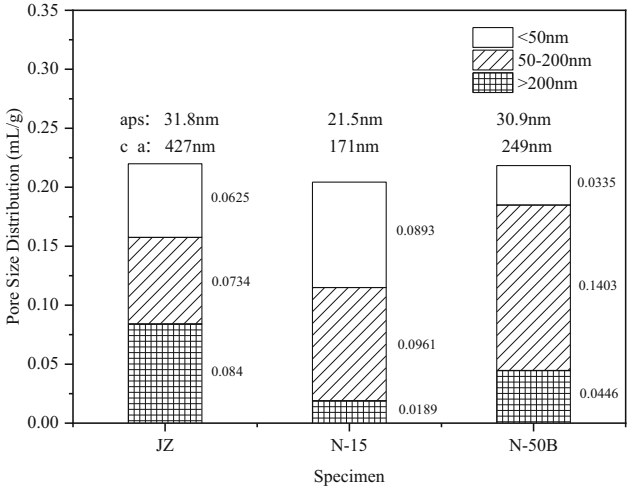

Figure 3: Pore structure distribution of specimens at 1 day. Note: aps = average pore size, ca = critical pore size.

have a greater effect on the microhardness than did 50 nm NS in the early stages.

3.4 Pore structure analysis

Wu and Lian [29] proved that voids with different sizes might have different effects on the permeability and durability of cement-based materials and classified the voids into three categories. Pores with diameters larger than 200 nm are harmful pores, mesopores with diameters between 50 and 200 nm are less harmful pores and pores with diameters below 50 nm are harmless pores.

The pore distribution, average pore size and critical pore size of different specimens at 1 day are shown in Figure 3. The results indicated that the average and critical pore size could be decreased with the incorporation of NS, and 15 nm NS presented a stronger effect on the pore size than did 50 nm NS. In particular, 15 nm NS could reduce the average and critical pore sizes from 31.8 and 427.0 nm to 21.5 and 171.0 nm, respectively, while 50 nm NS decreased the average and critical pore sizes to 30.9 and 249.0 nm, respectively. In addition, harmful pores declined significantly while less harmful pores increased significantly after adding NS. For example, 15 nm NS could reduce the harmful pores from 0.0840 to 0.0189 mL/g and increase the less harmful pores from 0.0734 to 0.0961 mL/g, while 50 nm NS decreased the harmful pores to 0.0446 mL/g and increased the less harmful pores to 0.1403 mL/g.

This was due to the filling effect and high activity effect of NS particles in the process of cement hydration; the tiny voids in the cement paste specimen could be filled well and the total porosity decreased. Furthermore, compared with equal amounts of 15 and 50 nm NS, 15 nm NS presented more effective results regarding pore size distribution and the average and critical pore size. This was because the smaller NS particles had a larger specific surface area, and more particles could form nuclei, which had a more powerful promoting effect on hydration. In addition, the smaller NS particles could more easily fill the pores so the structure was more compact and denser.

3.5 XRD analysis

The diffraction intensity of CH and C_3S peaks for each specimen at 1 day is shown in Figure 4. In addition, the content of C_3S in the cement paste after adding NS was lower than that of specimen JZ, particularly at 1 day. The diffraction peak lengths of specimens N-15, N-50A and N-50B were reduced by 7.7%, 27.1% and 24.7%, respectively, compared with that of specimen JZ at 1 day. Meanwhile, the diffraction peak length of CH of specimen N-15 was larger than those of the other specimens. This meant that 15 nm NS was more helpful for producing more CH in the early stage when compared with 50 nm NS.

Theoretically, CH crystals tend to have a crystalline plane (001) that is parallel to the interface. The orientation index of CH in this study was defined using data from XRD. According to the formula postulated by

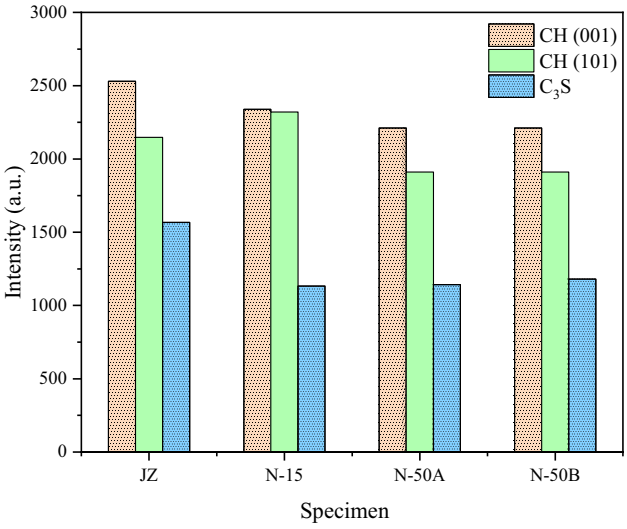

Figure 4: Diffraction intensity of CH and C_3S peaks for each specimen at 1 day.

Grandet and Olliver [30] and Azimah and Colin [31], the orientation index was defined as follows:

$$\text{Orientation index} = \frac{\text{Intensity (001)}}{\text{Intensity (101)} \times 0.74} \tag{2}$$

An index of unity represents a random arrangement, whereas an index greater than unity represents a CH orientation. The greater the orientation index, the stronger the orientation performance. The CH orientation index for each specimen at 1 day is shown in Figure 5. The results indicated that the incorporation of NS could reduce the orientation index of CH. Compared with that of specimen JZ at 1 day, the CH orientation index of specimens N-15, N-50A and N-50B were reduced by 0.23, 0.03 and 0.03, respectively. It seemed that smaller NS particles had a significant effect on the CH orientation, while the effect of larger NS particles was negligible.

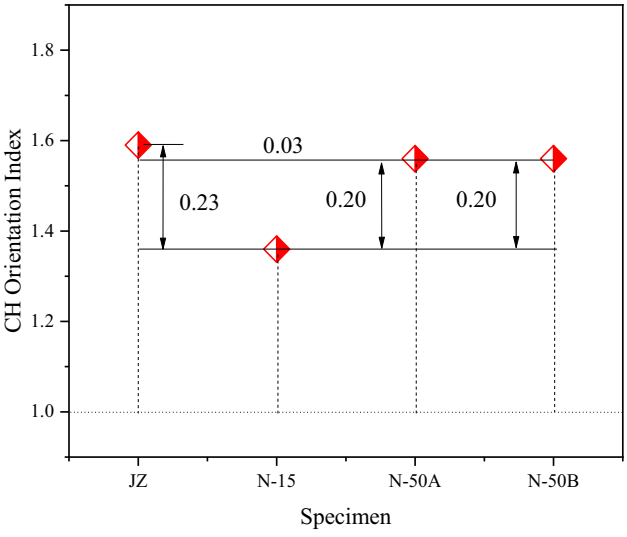

Figure 5: CH orientation index for each specimen at 1 day.

The cement paste with 15 nm NS had greater microhardness, a denser pore structure and a smaller CH orientation index than did the 50 nm NS, but the compressive strength was lower than that of the cement paste with 50 nm in the early stages. According to the formula postulated by Porter and Easteriing [27] and Muller [28], the nucleation rate (I) was defined as follows:

$$I = A \cdot N_T \cdot \exp\left(\frac{-\Delta G^*}{KT}\right) \tag{3}$$

where ΔG^* is the critical free energy for nucleation, T is the absolute temperature, K is the Boltzmann's constant, A is a constant and N_T is the number of nucleation sites.

When the crystal size of NS decreases, N_T tends to increase and ΔG^* shows a higher free energy. Under the influence of the exponential function, the declining value is far greater than the increase in N_T, which shows the general tendency of decline in I. Therefore, the velocity of C–S–H gel formation decreased, which caused the decrease in compressive strength.

3.6 DTA

The DTA curves of cement hydration for each specimen at 1 day are shown in Figure 6. Because the DTA in this study only focused on the change in CH, the temperature range of 400–500°C was analysed. The endothermic peak of CH around 460°C was analysed in this study.

The results indicated that the area of the endothermic peak of CH in the DTA curve was enhanced by NS, particularly 15 nm NS. Compared with that of specimen JZ, the heat absorption of specimen N-15 was increased by 71.70%, that of specimen N-50A was increased by 7.55% and that of specimen N-50B was increased by 35.85%. This demonstrated that cement hydration was promoted, and more CH was produced in the early stage with the incorporation of NS.

The endothermic peak of CH in specimen JZ was at approximately 461°C, and the position of the endothermic peak after incorporation of NS was shifted down to approximately 448°C. This indicated that the incorporation of NS could advance the endothermic peak of CH, which was because NS refined the CH grain [32]. This result was also consistent with that of the SEM image analysis.

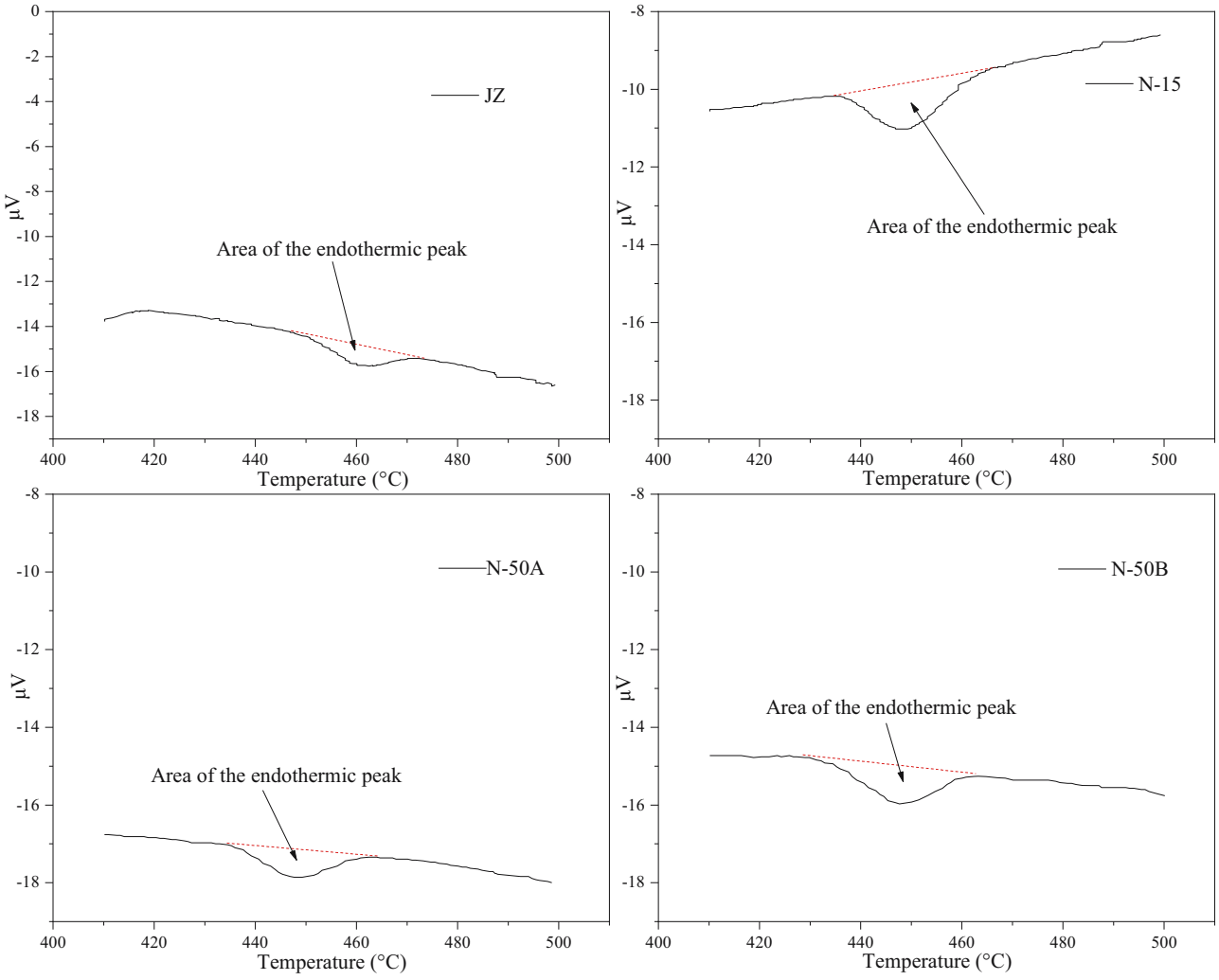

Figure 6: DTA curves of specimens at 1 day.

3.7 SEM analysis

The SEM images of the micromorphology of the cement paste at 1 day are shown in Figure 7, and images of the distribution of hydration products at 1 day are shown in Figure 8. The results revealed that there were more needle hydration products presented in the cement paste containing NS, which were in the form of stand-alone clusters, overlapped and joined together. The specimens with NS were more homogeneous, dense and compact when compared with the specimens without NS. This also demonstrated that NS promoted the early hydration of cement. The SEM images magnified by 20,000 times, as shown in Figure 7, showed that the incorporation of NS could produce more CH in the cement paste in the early stages. In addition, the incorporation of NS could also reduce the size of the CH crystals. This might have been due to the filling effect of NS, which reduced the growth space of CH crystals. The SEM images magnified by 40,000 times, as shown in Figure 8, showed that NS was attached to the surface of the C–S–H gel, which indicated that NS acted as a microaggregate and also played an important role in filling. Through the SEM analysis, the effect of NS on the hydration process of cement and the influence of the cement paste strength were qualitatively explained.

4 Conclusions

Mechanical properties and microhardness tests, MIP, XRD, SEM, and DTA, were employed in this study to determine the different effects and mechanisms of NS

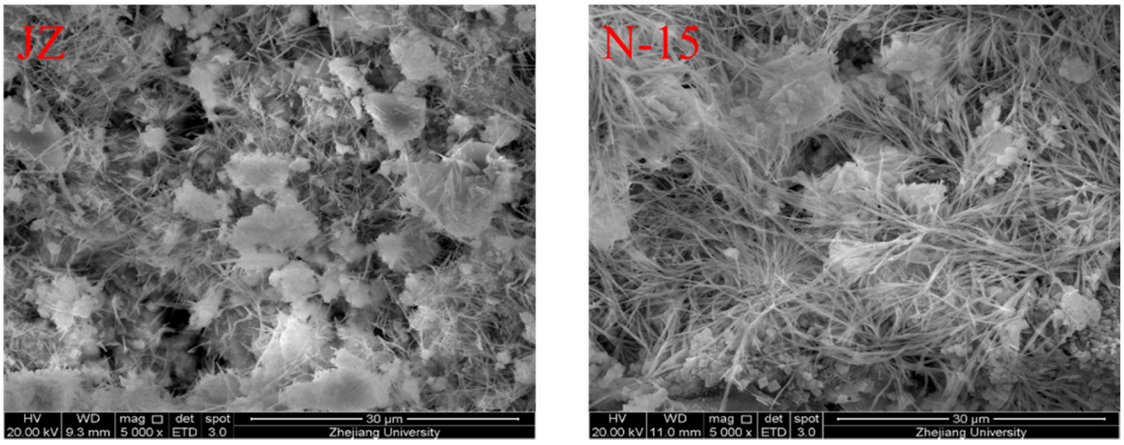

Figure 7: SEM images of specimens at 1 day.

with different particle sizes on cement pastes in the early stages.

1. The fluidity of the cement paste sharply decreased from 90 to 60 and 65 mm when 2.0% and 2.5% NS were added, respectively. This indicated that NS could significantly reduce the fluidity of the cement paste. The smaller particle size and greater NS content helped to greater reduce the fluidity.
2. The 50 nm NS showed a better performance for increasing the strength of cement-based materials

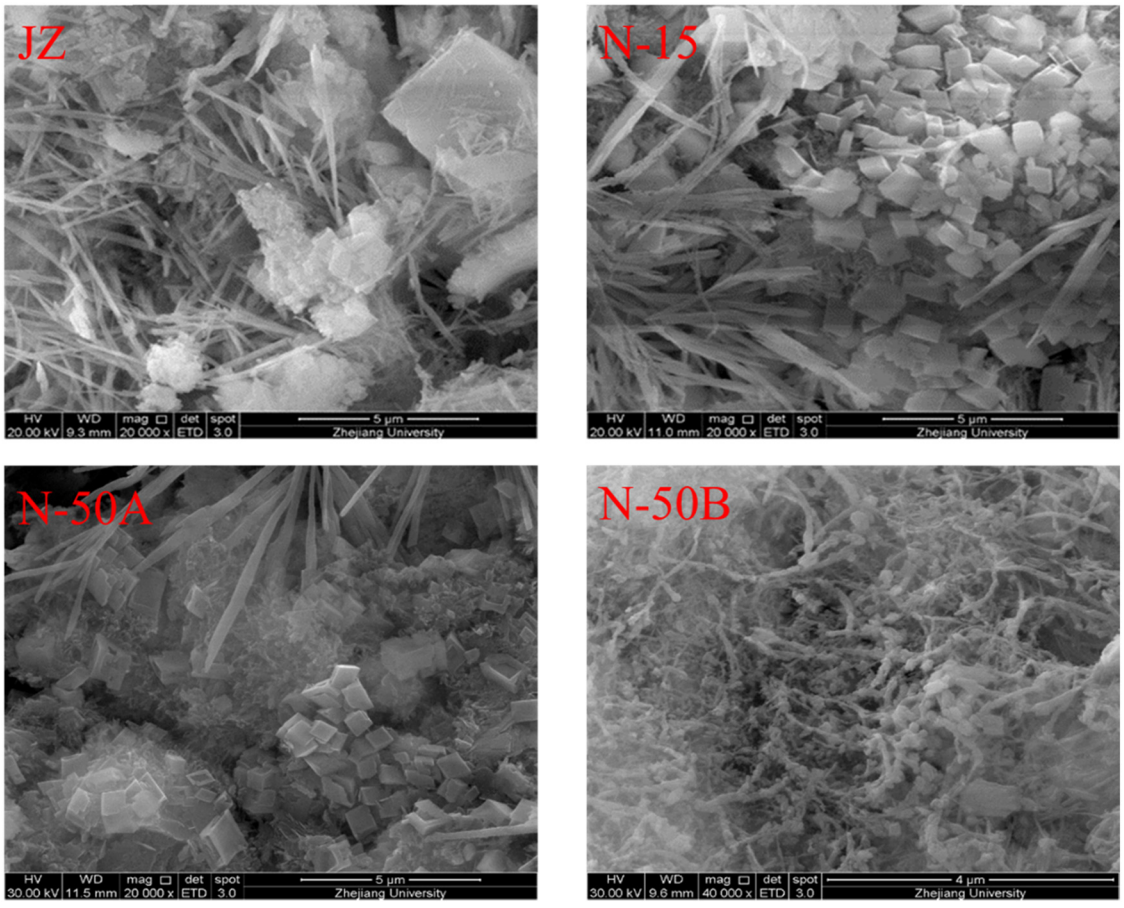

Figure 8: Main hydration products of specimens.

than did the 15 nm NS. The results showed that the compressive strengths of specimen N-50B were 14.6% and 11.0% higher than those of specimen N-15 at 1 and 28 days, respectively.

3. The 15 nm NS led to more positive behaviour for a denser microstructure of cement-based materials than did the 50 nm NS. The results indicated that the microhardness values of specimen N-15 were 17.7% and 14.0% higher than those of specimen N-50 at 1 and 3 days, respectively. In addition, 15 nm NS could reduce the average pore size from 31.8 to 21.5 nm, while 50 nm NS decreased the average pore size to 30.9 nm at 1 day.
4. The addition of NS promoted cement hydration and produced more CH in the early stages. Simultaneously, the value of the CH endothermic peak was advanced, and the CH grain was also refined when incorporated with NS.

After clarifying the early effects of NS with different particle sizes on cement-based materials, the application of nano-materials in the cement industry will be more reasonable. In conclusion, the particle size of nano-particles should be rationally selected according to the application. When high compressive strength of cement-based materials at early age is required in the engineering, larger NS particles should be selected. When the microstructure of cement-based materials is of greater concern, smaller NS particles are more suitable.

Acknowledgments: This work was financially supported by the National Defense Innovation Special Zone Project (18 163-13-ZT-007-003-01).

Conflict of interest: The authors declare no conflict of interest regarding the publication of this paper.

References

[1] Liu Y, Ong CN, Xie J. Emerging nanotechnology for environmental applications. Nanotechnol Rev. 2016;5(1):1–2.
[2] Norhasri MSM, Hamidah MS, Fadzil AM. Applications of using nano material in concrete: a review. Constr Build Mater. 2017;133:91–97.
[3] Ding K, Yang P, Cheng X. Surface treatment of cement-based materials using SiO_2 nanoparticles towards enhanced water absorption property. J Nanosci Nanotechnol. 2017;17:2067–71.
[4] Zhang P, Li Q-F, Wang J, Shi Y, Ling Y-F. Effect of PVA fiber on durability of cementitious composite containing nano-SiO_2. Nanotechnol Rev. 2019;8:116–27.
[5] Ahmed S, Meng T, Taha M. Utilization of red mud for producing a high strength binder by composition optimization and nano strengthening. Nanotechnol Rev. 2020;9:396–409.
[6] Quercia G, Hüsken G, Brouwers HJH. Water demand of amorphous nano silica and its impact on the workability of cement paste. Cem Con Res. 2012;42(2):344–57.
[7] Liu J, Li Q, Xu S. Influence of nanoparticles on fluidity and mechanical properties of cement mortar. Constr Build Mater. 2015;101:892–901.
[8] Senff L, Hotza D, Lucas S, Ferreira V, Labrincha J. Effect of nano-SiO_2 and nano-TiO_2 addition on the rheological behavior and the hardened properties of cement mortars. Mater Sci Eng A. 2012;532:354–61.
[9] Abd.El.Aleem S, Heikal M, Morsi WM. Hydration characteristic, thermal expansion and microstructure of cement containing nano-silica. Constr Build Mater. 2014;59:151–60.
[10] Afzali Naniz O, Mazloom M. Effects of colloidal nano-silica on fresh and hardened properties of self-compacting lightweight concrete. J Build Eng. 2018;20:400–10.
[11] Jo B, Kim C, Tae G, Park J. Characteristics of cement mortar with nano-SiO_2 particles. Constr Build Mater. 2007;21:1351–5.
[12] Sadeghi-Nik A, Berenjian J, Bahari A, Sattar A. Modification of microstructure and mechanical properties of cement by nanoparticles through a sustainable development approach. Constr Build Mater. 2017;155:880–91.
[13] Behfarnia K, Salemi N. The effects of nano-silica and nano-alumina on frost resistance of normal concrete. Constr Build Mater. 2013;48:580–4.
[14] Du H, Du S, Liu X. Durability performances of concrete with nano-silica. Constr Build Mater. 2014;73:705–12.
[15] Meng T, Zhang J, Wei H, Shen J. Effect of nano-strengthening on the properties and microstructure of recycled concrete. Nanotechnol Rev. 2020;9:79–92.
[16] Forood T, Elena R, Li W, Yaru S. Effects of nanosilica on early age stages of cement hydration. J Nanomater. 2017;2017:4687484.
[17] Du M, Jing H, Gao Y, Su H, Fang H. Carbon nanomaterials enhanced cement-based composites: advances and challenges. Nanotechnol Rev. 2020;9:115–35.
[18] Kooshafar M, Madani H. An investigation on the influence of nano silica morphology on the characteristics of cement composites. J Build Eng. 2020;30:101293.
[19] Xu Z, Zhou Z, Du P, Cheng X. Effects of nano-silica on hydration properties of tricalcium silicate. Constr Build Mater. 2016;125:1169–77.
[20] Land G, Stephan D. The influence of nano-silica on the hydration of ordinary Portland cement. J Mater Sci. 2012;47:1011–7.
[21] Haruehansapong S, Pulngern T, Chucheepsakul S. Effect of the particle size of nanosilica on the compressive strength and the optimum replacement content of cement mortar containing nano-SiO_2. Constr Build Mater. 2014;50:471–7.
[22] Givi A, Rashid S, Aziz F, Salleh M. Experimental investigation of the size effects of SiO_2 nanoparticles on the mechanical properties of binary blended concrete. Composites Part B. 2010;41:673–7.
[23] Givi AN, Rashid SA, Aziz FNA. Particle size effect on the permeability properties of nano-SiO_2 blended Portland cement concrete. J Compos Mater. 2011;45(11):1173–80.
[24] Haruehansapong S, Pulngern T, Chucheepsakul S. Effect of nanosilica particle size on the water permeability, abrasion resistance, drying shrinkage, and repair work properties of

cement mortar containing Nano-SiO_2. Adv Mater Sci Eng. 2017;152:1–11.
[25] China National Standards GB/T8077-2012, Methods for testing uniformity of concrete admixture, Beijing, China (in Chinese).
[26] China National Standards GB/T50081-2002, Standard for test method of mechanical properties on ordinary concrete, Beijing, China (in Chinese).
[27] Porter DA, Easteriing KE. Phase transformation in metals and alloys, 2nd edn. London: Chapman Hall; 1992. (ISBN 0 412 45030 5).
[28] Muller I. A history of thermodynamics – the doctrine of energy and entropy. Berlin, Germany: Springer; 2007. (ISBN-13 978-3-540-46226-2).
[29] Wu Z, Lian H. High performance concrete. Beijing, China: China Railway Publishing House; 1999. (ISBN: 9787113034580).
[30] Grandet J, Olliver JP. New method for the study of cement-aggregate interfaces. In: Seventh international Congress on Chemistry of Cement. vol. 3, Paris; 1980. p. 85–9.
[31] Azimah H, Colin P. Petrography evidence of the interfacial transition zone (ITZ) in the normal strength concrete containing granitic and limestone aggregates. Constr Build Mater. 2011;25:2298–303.
[32] Midgley HG. The determination of calcium hydroxide in set Portland cements. Cem Concr Res. 1979;9:77–82.